

## Micro Patterning of Crystalline Structures on a-ITO Films on Plastic Substrates Using Femtosecond Laser

Chung-Wei Cheng<sup>\*1</sup>, Wei-Chih Shen<sup>\*1</sup>, Yi-Ju Lee<sup>\*2</sup>, Jenq-Shyong Chen<sup>\*2</sup> and Chin-Wei Chien<sup>\*1</sup>

<sup>\*1</sup> ITRI South, Industrial Technology Research Institute, No. 8, Gongyan Rd., Liujia Shiang, Tainan County 734, Taiwan, R.O.C.

E-mail: CWCheng@itri.org.tw

<sup>\*2</sup> Department of Mechanical Engineering, National Chung Cheng University, No. 168, University Rd., Min-Hsiung, Chia-Yi 621, Taiwan, R.O.C.

It is well known that the resistivity and transparency of indium tin oxide (ITO) can be improved by utilizing a thermal annealing process to transform the original amorphous microstructure to a crystalline structure. However, the annealing process may result in irreversible damage to the underlying substrate; particularly if the substrate is fabricated from a plastic material. Accordingly, this study proposes a novel method for the fabrication of crystalline ITO (c-ITO) patterns on plastic substrates using femtosecond lasers with either a low (1 kHz) or a high (80 MHz) repetition rate. The resulting c-ITO patterns are observed using scanning electron microscopy (SEM). The results show that the pattern width varies logarithmically with the laser irradiation energy. In addition, it is shown that a high repetition rate is beneficial in suppressing the formation of micro-cracks on the surface of the c-ITO patterns.

**Keywords:** femtosecond laser, ITO, crystallization, plastic substrate

### 1. Introduction

In order to improve the device characteristics of optoelectronic products such as flat panel displays and solar cells, the amorphous materials used in their construction are transformed into crystalline materials via a thermal annealing process so as to reduce their resistivity and enhance their transparency. Amongst the various transparent conductive oxides (TCOs) used in the fabrication of optoelectronic products, indium tin oxide (ITO) is one of the most widely used due to its high transparency through the visible spectrum. Therefore, the problem of developing rapid and precise crystalline ITO (c-ITO) patterning techniques has attracted significant interest in recent years.

For ITO films deposited on glass substrates, the required c-ITO patterns are traditionally achieved by exposing the amorphous ITO (a-ITO) thin film using conventional photolithography methods and then processing the film using a thermal annealing technique [1]. In more recent studies, it has been shown that c-ITO patterns can be fabricated by using long-pulse (nanosecond) [2-9] or ultrafast pulse (picosecond or femtosecond) [10-12] lasers to ablate the undesired portion of the ITO thin films. However, long pulse lasers result in the formation of elevated ridges on either side of the pattern path and can cause significant damage to the underlying substrate. Moreover, even ultrafast pulse lasers do not necessarily prevent the formation of elevated ridges along the pattern path or the presence of ITO residue at the base of the ablated channel. Thus, much work remains to be done in identifying the optimal laser processing conditions for the patterning of c-ITO patterns for optoelectronic applications.

Recently, flexible plastic substrates have attracted tremendous attention for a wide range of applications, including flexible display, flexible solar cell, and so forth. How-

ever, plastic substrates cannot withstand temperatures greater than approximately 200°C. Accordingly, the ITO patterns within current flexible optoelectronic devices are necessarily fabricated using an amorphous (i.e. non-annealed) TCO. Consequently, the electrical and optical properties of such devices are inevitably somewhat lower than their glass-based counterparts. To resolve this problem, Chung et al. [13] proposed a method for crystallizing a-ITO thin films on plastic substrates using a nanosecond XeCl excimer laser (308 nm) and a thermal barrier layer. The results showed that the thermal barrier was successful in shielding the substrate from the laser energy. However, the proposed method required the use of a patterning mask, which not only complicated the patterning procedure, but also constrained the minimum attainable line pitch due to the optic diffraction limit of the mask. Legeay et al. [14] used scanning electron microscopy to observe the c-ITO patterns fabricated using the method presented in [13] and suggested that the cracks formed in the crystalline structures were the result of thermal shocks during the laser irradiation process.

This study proposes a novel two-step procedure for the fabrication of c-ITO patterns on plastic substrates without thermal barrier layers using a femtosecond laser-induced crystallization process. In the first step, the desired area of the ITO film is transformed from an amorphous structure to a crystalline structure via a laser irradiation process. In the second step, the relative difference in the etching rates of a- and c-ITO [15] is exploited to reveal the desired c-ITO patterns by etching the irradiated ITO films in an oxalic acid solution. The irradiation experiments are performed using two different femtosecond lasers (one low repetition rate and one high repetition rate) and various scanning speeds and laser powers. scanning electron microscopy

(SEM) observations are then performed to identify the optimal laser processing conditions.

## 2. Experimental

The irradiation experiments were performed using a-ITO thin films deposited on PET substrates. The experiments were conducted using two different femtosecond lasers, namely (1) a regenerative amplified mode-locked Ti:sapphire laser (SPIT FIRE, Spectra-Physics) with a low repetition rate of 1 kHz, a pulse duration of  $\sim 120$  fs, a central wavelength of 800 nm, and a maximum laser power of  $\sim 3.5$  W; and (2) an oscillator-only Ti:sapphire laser (Mai-Tai, Spectra-Physics) with a high repetition rate of 80 MHz, a pulse duration of  $\sim 100$  fs, a central wavelength of 800 nm, and a maximum laser power of  $\sim 225$  mW.

Figure 1 presents a schematic illustration of the experimental setup. To adjust the energy of the laser beam, the linearly polarized Gaussian beam emitted from the laser was attenuated by a rotatable half-wave ( $\lambda/2$ ) plate and a polarizing beam splitter (PBS). The transmitted component of the laser beam was then incident upon a beam splitter (BS), where the reflected beam was launched into a power detector in order to measure the laser irradiation energy. Meanwhile, the transmitted linearly polarized laser beam was passed through a shutter and a series of reflective mirrors such that it entered a 10x objective lens (numerical aperture 0.26, M Plan Apo NIR, Mitutoyo) in the normal direction on the surface of the ITO film. Note that the position of the objective lens was adjusted in the vertical (i.e. Z-axis) direction such that the focused spot had a diameter of  $\sim 5$   $\mu$ m for both femtosecond lasers.

The desired c-ITO patterns were fabricated by translating the sample stage in the X- and Y-directions under the control of a PC-based micro-positioning system with an accuracy of better than 1  $\mu$ m. The patterning process was monitored continuously using a charge-coupled device (CCD) camera. After the irradiation process, the samples were immersed in a 0.1 N oxalic acid etchant solution at 50  $^{\circ}$ C for 2 min. Finally, the etched samples were observed using SEM (FE-SEM 7001).

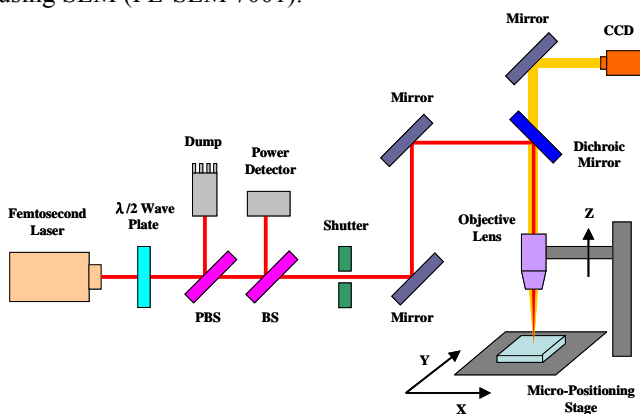
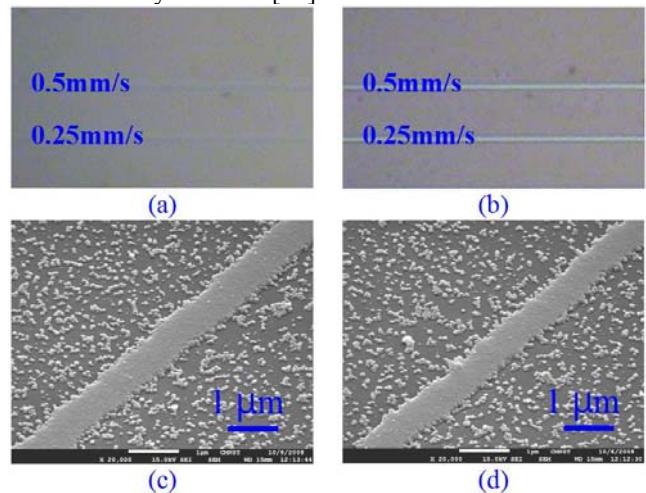


**Fig. 1** Schematic illustration of femtosecond laser irradiation system

## 3. Results and Discussion

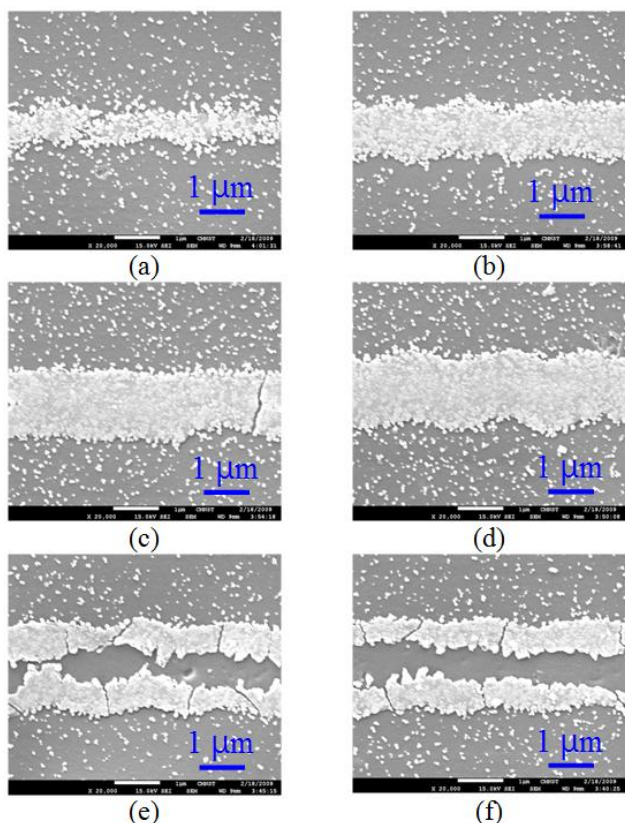
### 3.1 Irradiation experiments using low repetition rate femtosecond laser (1 kHz)

Figure 2(a) presents a microscope image showing the line patterns fabricated on an a-ITO thin film surface using a laser power of 85  $\mu$ W (85 nJ) and scanning speeds of 0.25 and 0.5 mm/s, respectively. Note that the specimen is in an unetched condition. It can be seen that the film within the laser-irradiated area is slightly different from that within the unirradiated region. The irradiated sample was then etched, leaving clear line patterns on the substrate, see Fig. 2(b). Figures 2(c)–(d) present SEM images of the line patterns from Fig. 2 (b). In every case, the lines are found to have a width of around 1.1  $\mu$ m. This result indicates that the etching rate of the laser-irradiated line pattern is much lower than that of the a-ITO thin film, and thus the unirradiated ITO is removed without any significant erosion of the irradiated ITO patterns. The irradiated ITO pattern is presumed to be crystalline since the etching rates of a- and c-ITO are very different [15].



**Fig. 2** (a)–(b) Microscope images of irradiated a-ITO thin film surfaces before and after etching, respectively. (c)–(d) SEM images showing line patterns fabricated at different scanning speeds, i.e. (c) 0.25mm/s and (d) 0.5mm/s.

Figures 3 and 4 present SEM images of the c-ITO line patterns fabricated using laser powers in the range 80–90  $\mu$ W and scanning speeds of 0.25 mm/s and 0.5 mm/s, respectively. Since the laser beam has a Gaussian profile, the middle of the line is irradiated by a higher intensity than the outer edges. In the c-ITO line patterns shown in Figs. 3(a)–(d), the peak energy intensity of the laser beam is higher than the crystallization threshold, but is lower than the ablation threshold. As a result, a crystallization of the a-ITO layer takes place, but no ablation effect is observed. As shown in Figs. 3(e)–(f), corresponding to laser powers of 88  $\mu$ W and 90  $\mu$ W, respectively, the center of the line is ablated, which indicates that the peak energy intensity of the laser beam is higher than the ablation threshold. However, due to the Gaussian nature of the laser beam profile, the outer edges of the line are subject to a lower irradiation intensity, and thus the ablated channels are bordered on either side by a thin strip of crystalline ITO. Comparing Figs. 3(e) and 4(e), it is observed that an ablation effect is induced only at the lower scanning rate since under these conditions, the focus area on the ITO surface is irradiated by a greater number of laser pulses and thus the ablation threshold of the a-ITO material is reduced accordingly.



**Fig. 3** SEM images of c-ITO line patterns fabricated with scanning speed of 0.25 mm/s and laser powers of (a) 80  $\mu$ W, (b) 82  $\mu$ W, (c) 84  $\mu$ W, (d) 86  $\mu$ W, (e) 88  $\mu$ W and (f) 90  $\mu$ W

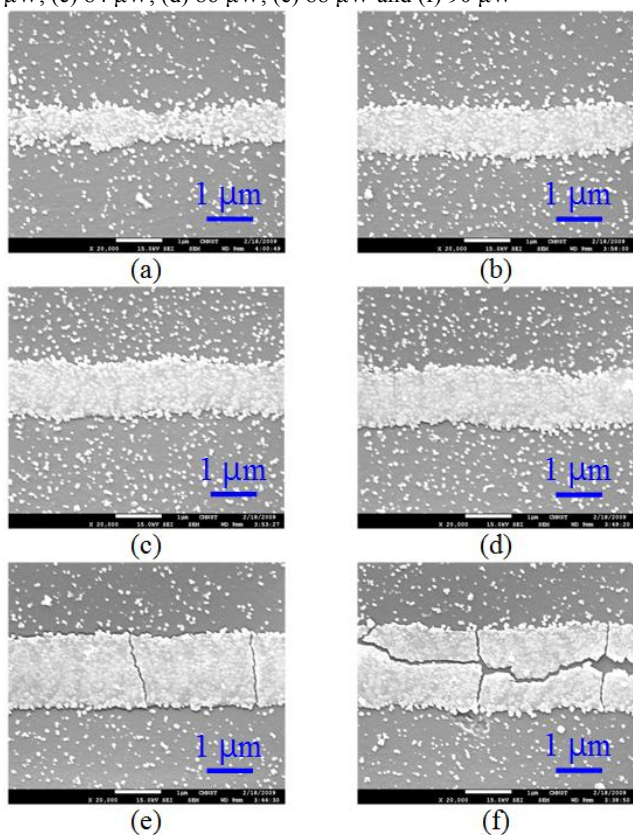


**Fig. 4** SEM images of c-ITO line patterns fabricated with scanning speed of 0.5 mm/s and laser powers of (a) 80  $\mu$ W, (b) 82  $\mu$ W, (c) 84  $\mu$ W, (d) 86  $\mu$ W, (e) 88  $\mu$ W and (f) 90  $\mu$ W

In Figures 3 and 4, it can be seen that the widths of the crystallized patterns are sensitive to the spatial intensity distribution of the focused laser beam. Assuming a Gaussian incident beam profile, the pattern width  $W$  is related to the irradiation laser energy  $E$  by

$$W^2 = 2\omega_e^2 \ln(E/E_{th}) \quad (1)$$

where  $E_{th}$  is the multiple pulse crystallization threshold energy and  $\omega_e$  is the effective beam radius at the interaction surface. Figure 5 plots the variation of the measured crystallization pattern width as a function of the laser energy for scanning speeds of 0.25 mm/s and 0.5 mm/s, respectively. The straight lines obtained by curve fitting the experimental data confirm the logarithmic dependence between the pattern width and the irradiation energy. Moreover, the annealing threshold is estimated to be around 77 nJ. It is observed that a lower scanning speed (i.e. a greater number of laser pulses applied to the same spot) results in a lower crystallization threshold energy. This result is most reasonably attributed to the incubation phenomenon reported in [16]. Finally, the slope of the fitting line is found to be around 11.1 for both scanning speeds and the effective beam diameter was determined to be 4.7  $\mu$ m, i.e. similar to the theoretical focus spot size 5  $\mu$ m.

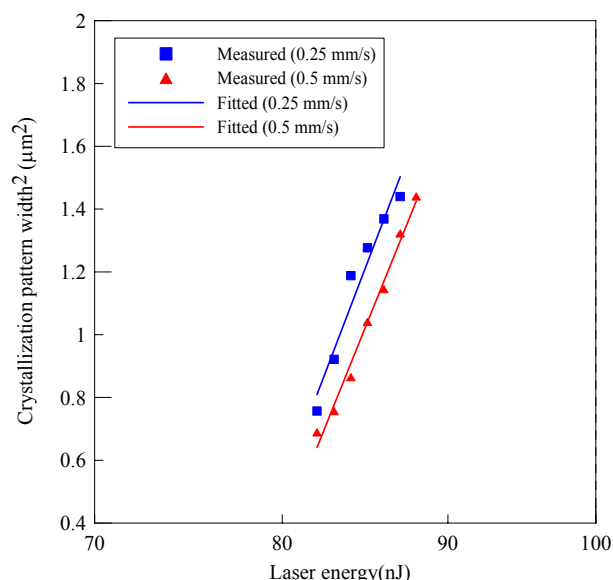


**Fig. 5** Variation of pattern width with laser energy as function of scanning speed

### 3.2 Irradiation experiments using high repetition rate femtosecond laser (80 MHz)

Figure 6 presents SEM images of the c-ITO line patterns created by the high repetition rate femtosecond laser at a scanning speed of 1.0 mm/s and laser powers in the range 213–225 mW. It is evident that the micro-cracks observed in the c-ITO line patterns in Figs. 3–4 are no longer present. Thus, it appears that the high repetition rate femtosecond laser is beneficial in producing a more uniform crystallization effect than that produced by the low repetition rate laser. Note that the laser beam was focused at a position 100  $\mu$ m above the surface of the a-ITO film in order to reduce the thermal effect at the PET substrate and the interface of ITO film and PET substrate [17]. However, the defocus method will decrease the energy density for the

same laser power and limit the highest scanning speed. The processing speed could be further improved by using high power laser source.

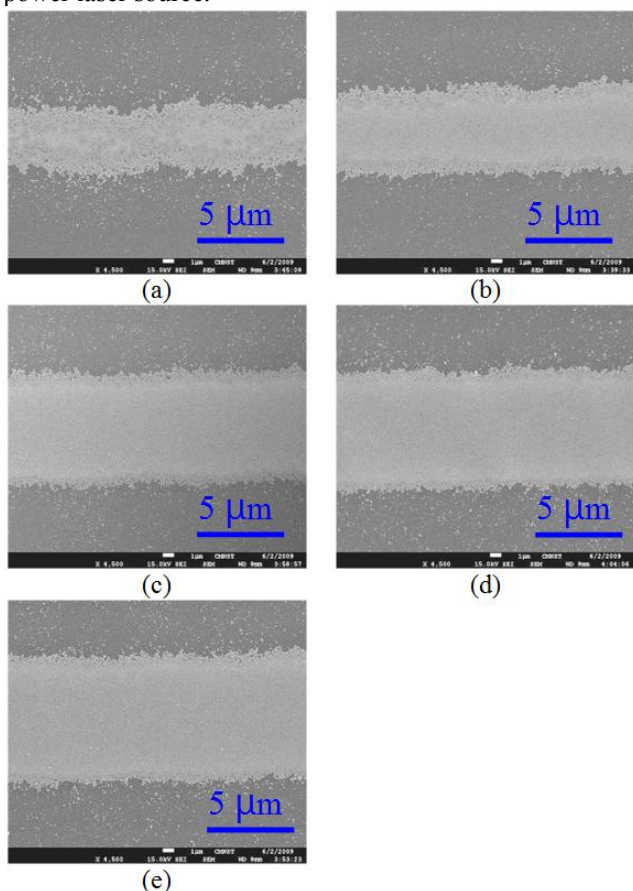


**Fig. 6** SEM images of c-ITO line patterns fabricated with scanning speed of 1.0 mm/s and laser powers of (a) 213 mW, (b) 216 mW, (c) 219 mW, (d) 222 mW and (e) 225 mW.

Gattass et al. [18] reported that the use of high repetition rate ( $> 200$  kHz) femtosecond lasers in processing certain bulk transparent glasses results in a heat accumulation effect which minimizes the thermal cycling between successive laser pulses and therefore suppresses collateral damage. The crack-free appearance of the c-ITO patterns presented in Fig. 6 suggests that the current 80 MHz repetition rate femtosecond laser induces a similar heat accumulation effect. The effective cooling time of a-ITO is given by  $t_c = d_v^2/D$ , where  $d_v$  is the diameter of the laser beam on the sample surface and  $D$  is the thermal diffusivity of a-ITO and has a value of approximately  $1.2 \times 10^{-6}$  m<sup>2</sup>/s [19]. In the current experiments, the  $d_v$  is equal to approximately 25  $\mu$ m, and thus the effective cooling time of the ITO film is around 525  $\mu$ s. This value of  $t_c$  is much larger than the interval between successive pulses, i.e. 0.012  $\mu$ s for an 80 MHz repetition rate. As a consequence, a significant heat accumulation effect occurs within the focus spot region, and thus the effects of collateral damage (i.e. micro-cracks) are effectively suppressed.

Figure 7 shows the variation of the measured pattern width as a function of the laser irradiation energy for scanning speeds of 0.5 and 1 mm/s, respectively. The straight line obtained by curve fitting the experimental measurements again confirms the logarithmic dependence of the pattern width on the laser irradiation energy, as shown in

Eq. (1). Note that in this case, however, the effective beam radius term  $\omega_e$  in Eq. (1) is replaced by  $\omega_{e,h}$ , which is equal to the approximate summation of the focused beam radius and the extended width caused by the heat accumulation effect. From an inspection of Fig. 7, a lower scanning speed results in a lower annealing threshold energy. The slope of the fitting line is found to be around 1247 for scanning speed 0.5 mm/s. Furthermore, the effective beam diameter was determined to be around 50  $\mu$ m.

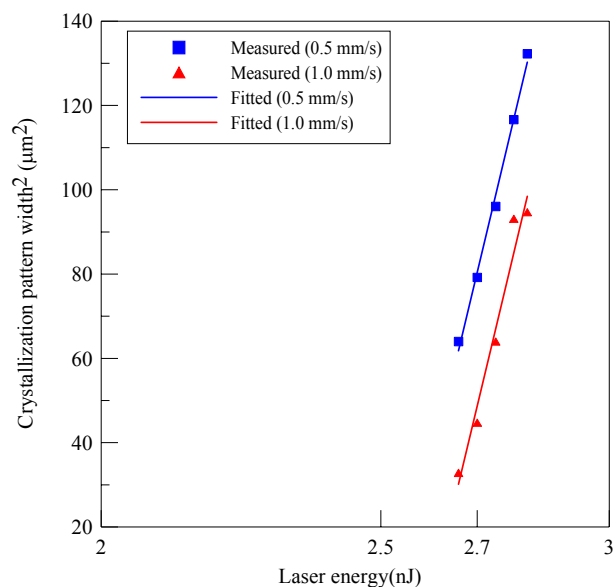


**Fig. 7** Variation of pattern width with laser energy as function of scanning speed

#### 4. Conclusions

This study has proposed a novel femtosecond laser-induced crystallization process for the patterning of high quality c-ITO structures on plastic substrates without a thermal barrier layer. In general, the results have shown that the c-ITO pattern width can be adjusted through a careful control of the laser power. In addition, it has been shown that the surface quality of the c-ITO patterns can be improved via the use of a high repetition rate (80 kHz) femtosecond laser. Overall, the proposed technique enables the fabrication of highly-precise c-ITO patterns with no discernible damage to the underlying substrate. As a result, it provides an ideal solution for the patterning of the micro-electrodes used in optoelectronic devices fabricated on plastic substrates.

#### Acknowledgements

The authors would like to appreciate the support from the Ministry of the Economic Affairs (MOEA), Taiwan, R.O.C. for performing this project.

#### References

- [1] H. Morikawa and M. Fujita, "Crystallization and electrical property change on the annealing of amorphous indium-oxide and indium-tin-oxide thin," *Thin Solid Films*, Vol. 359, 2000.
- [2] O. Yavas et al., "Effect of substrate absorption on the efficiency of laser patterning," *J. Appl. Phys.*, Vol. 85, 1999.

- [3] R. Tanaka et al., "Laser etching of indium tin oxide thin films by ultra-short pulsed laser," Proc. of SPIE, Vol. 5063, 2003.
- [4] D. Ashkenasi et al., "Fundamentals and advantages of ultrafast micro-structuring of transparent materials," Appl. Phys. A 77, 2003.
- [5] C. Molpeceres et al., "Microprocessing of ITO and a-Si thin films using ns laser sources," J. Micromech. Microeng., Vol. 15, 2005.
- [6] J.H. Kim, "The analysis of ablation on ITO thin film for 1064nm irradiation," Proc. of the 4th International Congress on Laser Advanced Materials Processing, 2006.
- [7] N. Fukuda, "Development of DPSS-laser-based ITO patterning system," ICALEO Congress Proceeding, 2006.
- [8] M. Henry et al., "Laser direct write of active thin-films on glass for industrial flat panel display manufacture," Proc. of the 4th International Congress on Laser Advanced Materials Processing, 2006.
- [9] M.Y. Xu et al., "F<sub>2</sub>-laser patterning of indium tin oxide (ITO) thin film on glass substrate," Appl. Phys. A, Vol. 75, 2006.
- [10] M. Park et al., "Ultrafast laser ablation of indium tin oxide thin films for organic light-emitting diode application," Optics and Lasers in Engineering, Vol. 44, 2006.
- [11] I.B. Sohn et al., "Femtosecond laser patterning of ITO film for display panel," Proc. of the 4th International Congress on Laser Advanced Materials Processing, 2006.
- [12] Gediminas RAČIUKAITIS et al., "Patterning of ITO layer on glass with high repetition rate picosecond lasers," Journal of Laser Micro/Nanoengineering, Vol. 2, 2007.
- [13] W. Chung et al., "Room temperature indium tin oxide by XeCl excimer laser annealing for flexible display," Thin Solid Films, Vol. 460, 2004.
- [14] G. Legeay et al., "Excimer laser beam/ITO interaction: from laser processing to surface reaction," Phys. Stat. Sol., Vol. 5, 2008
- [15] J.E.A.M. van den Meerakker, et al., "On the homogeneity of sputter-deposited ITO films Part II. Etching behavior," Thin Solid Films, Vol. 266, 1995.
- [16] D.V. Tran et al., "Quantification of thermal energy deposited in silicon by multiple femtosecond laser pulses," Opt. Express, Vol. 14, 2006.
- [17] D.A. Willis, "Thermal mechanisms of laser micromachining of indium tin oxide," Proc. of SPIE, Vol. 5339, 2004.
- [18] R.R. Gattass et al., "Micromachining of bulk glass with bursts of femtosecond laser pulses at variable repetition rates," Opt. Express, Vol. 14, 2006.
- [19] S. Juodkakis et al., "Thermal accumulation effect in three-dimensional recording by picosecond pulses," Appl. Phys. Lett., Vol. 85, 2004.

(Received: June 17, 2009, Accepted: October 26, 2009)